A Twist on Facial Selectivity of Hydride Reductions of Cyclic Ketones: Twist-Boat Conformers in Cyclohexanone, Piperidone, and Tropinone Reactions

Sharon R. Neufeldt,[†] Gonzalo Jiménez-Osés,*,[†] Daniel L. Comins,*,[‡] and K. N. Houk*,[†]

[†]Department of Chemistry and Biochemistry, University of California, Los Angeles, California 90095, United States
[‡]Department of Chemistry, North Carolina State University, Raleigh, North Carolina 27695-8204, United States

Ⓢ *Supporting Information*

ABSTRACT: The role of twist-boat conformers of cyclohexanones in hydride reductions was explored. The hydride reductions of a cis-2,6-disubstituted *N*-acylpiperidone, an *N*-acyltropinone, and *tert*-butylcyclohexanone by lithium aluminum hydride and by a bulky borohydride reagent were investigated computationally and compared to experiment. Our results indicate that in certain cases, factors such as substrate conformation, nucleophile bulkiness, and remote steric features can affect stereoselectivity in ways that are difficult to predict by the general Felkin−Anh model. In

particular, we have calculated that a twist-boat conformation is relevant to the reactivity and facial selectivity of hydride reduction of cis-2,6-disubstituted *N*-acylpiperidones with a small hydride reagent (LiAlH$_4$) but not with a bulky hydride (lithium triisopropylborohydride).
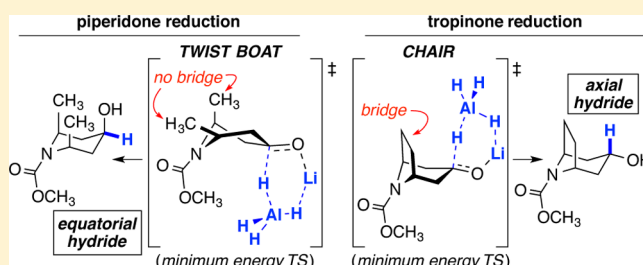
■ INTRODUCTION

Stereoselectivity of Hydride Reductions of Cyclohexanones. Nucleophilic additions to conformationally biased cyclohexanones can provide two stereoisomeric alcohol products via reaction at the "axial" or the "equatorial" face of the carbonyl (Figure 1). The factors controlling selectivities
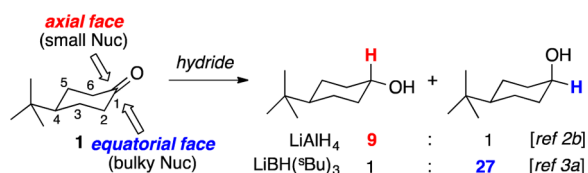

Figure 1. Facial selectivity of hydride addition to 4-*tert*-butylcyclohexanone **1**.

have been studied and debated for roughly three-quarters of a century.[1] The facial selectivity of addition is influenced by the size of the nucleophilic reagent: small nucleophiles tend to add to the axial face, whereas bulky nucleophiles preferentially attack the equatorial face. For example, NaBH$_4$[2a] and LiAlH$_4$[2b] both deliver hydride to the axial face of 4-*tert*-butylcyclohexanone (**1**), giving an equatorial alcohol as the major product, whereas bulky hydride reagents such as LiHB^{s}Bu$_3$ (L-Selectride)[3] preferentially yield the axial alcohol via equatorial hydride delivery (Figure 1).

The observed preferential addition of bulky reagents to the equatorial face is generally attributed to steric factors: the axial face is more hindered than equatorial due to 1,3-diaxial

interactions with the incoming nucleophile.[4] Historically, this was termed "steric approach control" by Dauben.[4a] Conversely, Dauben attributed the axial preference observed with smaller reagents to "product development control", reflecting the greater stability of the resulting equatorial alcohol. A more widely accepted model based on torsional strain was first proposed by Felkin and later supported computationally by Anh and Eisenstein.[5] This so-called Felkin−Anh model posits that the transition state (TS) for addition to the equatorial face of a cyclohexanone chair involves torsional strain greater than that of axial attack; that is, there are more eclipsing interactions during equatorial attack compared to axial (Figure 2). The
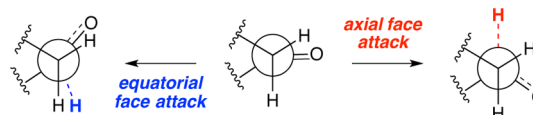

Figure 2. Increased eclipsed interactions (torsional strain) in equatorial face attack of hydrides to carbonyl compounds.

stereoelectronic basis of these facial preferences has been studied extensively through computational methods by Houk[6] and others[7] using small hydride reagents (LiH, NaBH$_4$, LiAlH$_4$) as computationally affordable systems. Although other models have been proposed, including Cieplak's model that emphasizes overlap between an antiperiplanar σ orbital and the developing

σ^* orbital,[8] theoretical studies using small hydride reagents[6] overall support the torsional strain model.

Hydride Reductions of *N*-Acylpiperidones. This general trend in facial selectivity does not hold, however, for some six-membered cyclic ketones. Cis-2,6-disubstituted *N*-acylpiperidones (e.g., compounds **2** and **3** in Scheme 1) have been

Scheme 1. Facial Selectivities of Hydride Addition to Piperidones and Tropinones
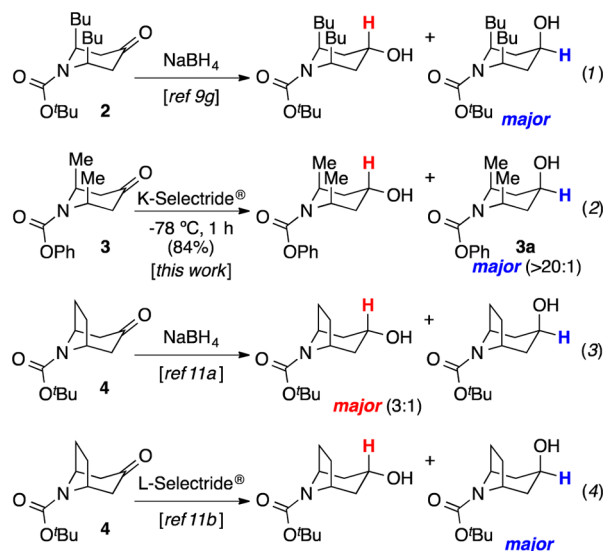
studied extensively by the Comins group[9a−f] and others.[9g] For **2** and **3**, hydride addition from the equatorial face is favored even when a small hydride reagent (NaBH₄) is used (Scheme 1, eqs 1 and 2). Indeed, the axial face of this class of substrates should be particularly hindered due to the axial 2,6-substituents, forced into this conformation by $A^{1,3}$ strain with the N-substituent.[10] Surprisingly, however, the more conformationally restricted bridged analogues (tropinones, e.g., compound **4**) undergo favored axial attack by small hydride reagents despite the steric hindrance imposed by the bridge (eqs 3 and 4).[11]

Low energy twist-boat conformations of piperidones have been observed in solution by NMR spectroscopy and in the solid state by X-ray diffraction.[11] We wondered if these twist-boat conformers might be relevant to the transition states of reactions of these compounds. To study this possibility experimentally, we compared the reactivity of piperidone **3** and its tropinone analogue **5** toward K-Selectride. Notably, although the former substrate can access a twist-boat conformation, the latter cannot due to geometrical constraints. Based on the results of a competition experiment (Scheme 2), the rate of reduction of tropinone **5** with K-Selectride is about

Scheme 2. Competition Experiment between Piperidone 3 and Tropinone 5 for Reduction with K-Selectride
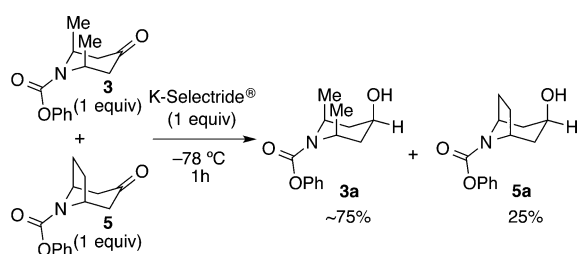
3-fold slower than that of piperidone **3**; however, both processes are completely selective toward formation of the axial alcohol (equatorial attack of hydride). This result, in combination with the contrasting stereoselectivity of these two classes of substrates with nonbulky hydrides (Scheme 1, eqs 3 and 4),[9,11] encouraged us to computationally explore the hypothesis that a twist-boat transition state could in fact be contributing significantly to the reaction of cis-2,6-disubstituted *N*-acylpiperidones.[12]

We have undertaken a computational study of the factors influencing the differences in reactivity and facial selectivity of reduction of these two structurally similar piperidone and tropinone substrate classes. We have analyzed the roles of the six-membered ring conformation and the size of the nucleophile on stereoselectivities. The contributions of both steric repulsion and torsional strain to the activation energy upon hydride addition, factors that have been found to be particularly relevant in cyclic ketones,[13] were analyzed. Our calculations indicate that, although a chair conformation experiences greater torsional strain during attack at the equatorial face by a small hydride, attack at the two faces of a twist-boat do not necessarily follow the same trend. Additionally, with very bulky hydride reagents, the difference in torsional strain during attack at the axial vs equatorial face of a chair is nearly negligible due to a late transition state.

■ RESULTS AND DISCUSSION

Figure 3 depicts the substrates and hydride reagents used in our computational studies. While 4-*tert*-butylcyclohexanone (**1**) is a
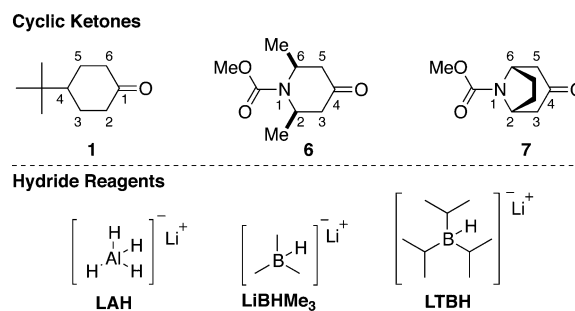
Figure 3. Cyclic ketone substrates and hydride reagents considered in this work.

well-studied conformationally biased cyclic ketone, chosen as a baseline, *N*-methoxycarbonyl-*cis*-2,6-dimethylpiperidone (**6**) and *N*-methoxycarbonyltropinone (**7**) were selected as piperidone and tropinone model substrates.

Lithium aluminum hydride (LAH) is the small hydride model. For a bulky hydride, we mimicked the reactivity of L-Selectride (lithium tri-*sec*-butylborohydride) using a computationally affordable surrogate (L-Selectride is conformationally and stereochemically very complex, with thousands of low energy conformers).[14] We initially tested LiBHMe₃ as a bulky hydride model but were unable to reproduce the experimental selectivities using this relatively simple trialkylborohydride. However, a more sterically demanding hydride, lithium triisopropylborohydride (LTBH) was found to satisfactorily reproduce the experimental selectivities of L-Selectride, albeit at greater computational cost than LiBHMe₃ due to the large conformational space of LTBH. Some comparisons with K-Selectride are made as well.
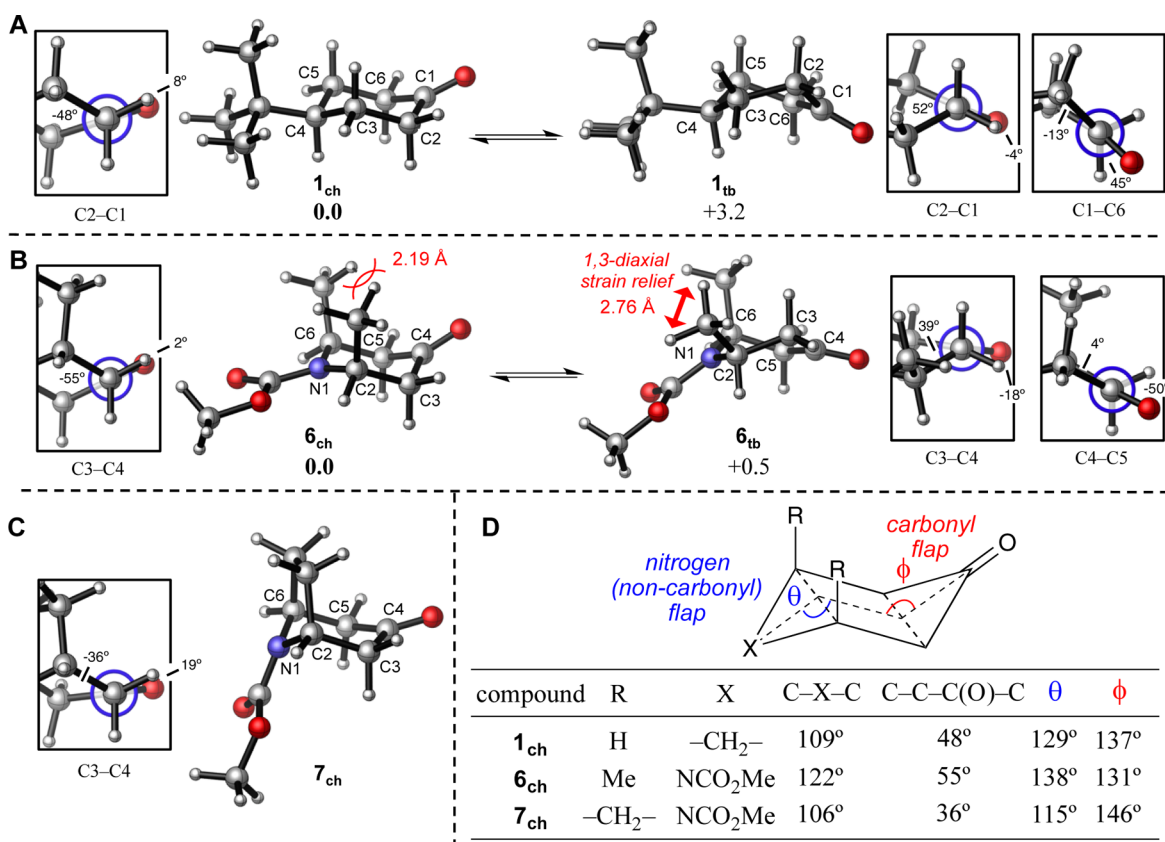
Figure 4. Conformations of cyclic ketone substrates calculated at the SMD(THF)/B3LYP/6-311+G(2d,p)//B3LYP/6-31G(d,p) level. Gibbs free energies (ΔG) are referenced to the lowest energy conformer, when applicable, and are given in kcal mol^{-1}; angles are given in degrees.

Conformations of Starting Reactants. Figure 4 depicts the calculated geometries of the most stable chair (1_{ch}, 6_{ch}, and 7_{ch}) and twist-boat (1_{tb} and 6_{tb}) conformations of the cyclic ketone substrates. Newman projections sighting down the ring carbon–carbonyl carbon bond are also provided. Because of an internal plane of symmetry in the chair conformations, the two possible Newman projections are enantiomeric (e.g., sighting down the C2–C1 bond of 1_{ch} provides the mirror image of sighting down C6–C1). Conversely, two different Newman projections are given for 1_{tb} and 6_{tb}, as the twist-boat conformations of these substrates lack a plane or axis of symmetry.

In the ground state, **1** adopts a chair conformation (1_{ch}) that is more stable than the minimum energy twist-boat conformation (1_{tb}, in which C1 and C4 are at the bow and stern) by 3.2 kcal mol^{-1} (Figure 4A).

Both chair and twist boat conformations were also located for piperidone **6** (Figure 4B). Previous studies on cis-2,6-disubstituted *N*-acylpiperidones have indicated that the chair conformation with equatorial 2- and 6-substituents is unstable.[9g,15] The resulting $A^{1,3}$-strain between the 2,6-diequatorial and the N-substituents disfavors such a conformation, and instead these substituents exist in an axial (or pseudoaxial) orientation in conformation 6_{ch}. Indeed, our calculations show that the energy penalty for placing these two groups equatorial is 6.1 kcal mol^{-1} relative to 6_{ch} (see Supporting Information). Despite the greater intrinsic stability of chair conformations, 6_{ch} has a disadvantageous 1,3-diaxial interaction between the two axial methyl substituents, which is alleviated in 6_{tb} (the distances between the proximal hydrogens of the two methyl groups in 6_{ch} and 6_{tb} are 2.19 and 2.76 Å, respectively). The

calculated geometry of the most stable 6_{tb} very closely matches that predicted by the NMR studies of Venkatraj et al., in which C6 (the ring carbon syn to the carbonyl of the *N*-acyl group) and C3 are at the bow and stern positions.[15] The twist-boat conformation of **6** is predicted to be only 0.5 kcal mol^{-1} higher in energy than 6_{ch}, suggesting the coexistence of both isomers in solution. As described above, previous experimental and computational studies have indicated that similar piperidones (albeit bearing bulkier 2- and 6-substituents) exist predominantly in a twist-boat conformation in solution and in the solid state.[9a,15,16]

The six-membered ring of tropinone **7** is locked into a chair conformation (Figure 4C). The bridging $-CH_2CH_2-$ cinches the chair together on one side, making the nitrogen flap more folded in 7_{ch}, with a flap angle (out-of-plane dihedral angle) of 115° compared to 138° in 6_{ch} (θ, Figure 4D). Conversely, the carbonyl flap on the opposite side of 7_{ch} is more flattened, with a flap angle of 146° (ϕ, Figure 4D), compared to 131° in 6_{ch} and 137° in 1_{ch}.

Reactivity with LAH. The lowest energy reactant species for the reduction of cyclic ketones **1**, **6**, and **7** by LAH are prereaction coordination complexes that are stabilized by −10.9 to −12.3 kcal mol^{-1} with respect to the separated reactants (see, for example, Figure 5A). Substrate geometries are not significantly distorted by formation of the coordination complexes, and the energy differences between chair and twist-boat conformations (for **1** and **6**) are very nearly conserved (Figure 5B). Thus, all of the calculated activation barriers reported herein are measured from the lowest-energy prereaction coordination complexes. Although the most realistic representation of the lithium counterion would likely
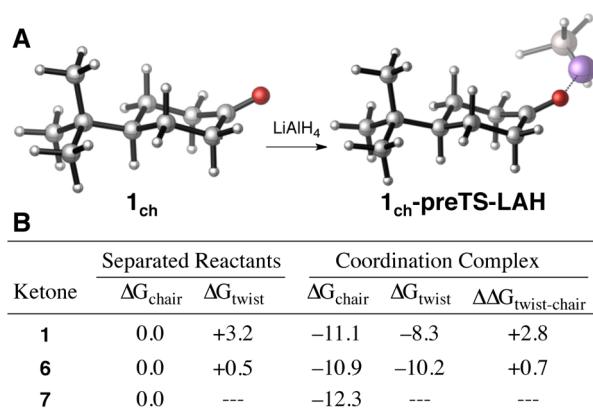
Figure 5. (A) Example of formation of the reactant complex with LAH, shown for 1_{ch}. (B) Comparison of the Gibbs free energies (ΔG) of chair and twist-boat conformations of free ketones **1**, **6**, and **7** and their prereaction complexes with LAH. Optimized structures were calculated at the SMD(THF)/B3LYP/6-311+G(2d,p)//B3LYP/6-31G(d,p) level. Gibbs free energies (ΔG) are referenced to the lowest energy free ketone conformation and are given in kcal mol^{-1}.

include coordinated solvent (THF) molecules, we were unable to obtain optimized geometries of all the transition states needed to account for stereoselectivity using explicit solvent. However, significant computational precedent exists for successfully reproducing experimental selectivities of hydride reductions involving nonexplicitly solvated lithium species.[6,7]

Because neither face of a twist-boat experiences nucleophilic attack via a true axial or equatorial trajectory, attack on the twist-boat face that corresponds to the axial face of the analogous chair will be herein be referred to as "pro-axial" attack or attack at the "pro-axial face" (the term "pro-equatorial" will also be used). These terms refer to the orientation of the added nucleophile in the product (i.e., the axial or equatorial orientation of the hydride) and not of the hydroxyl. The torsional strain associated with the transition states herein is represented graphically by Newman projections and described numerically by the parameter ψ, which corresponds to the average deviation from 60° of the 12 dihedral angles of both Newman projections involving the carbonyl carbon (Figure 6). It should be noted that due to the
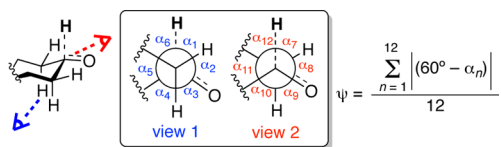

Figure 6. Measurement of torsional strain (ψ) in the TS of hydride addition to cyclic ketones.

intrinsic conformational differences between chair and twist-boat conformations, there is a certain amount of eclipsing already associated with the twist-boats. Hence, the ranges of ψ values for these two ring conformers are different, and these parameters should only be compared between attack at the axial and equatorial faces of the same ring conformation, not across different conformations. It should be also noted that, depending on the position of the TS in the reaction coordinate, the range of values for ψ can change significantly due to the greater sp^3 character of the carbonyl carbon in late and more distorted TS.

The transition structures obtained for addition of LAH to both faces of the different conformations of ketones **1**, **6**, and **7** are provided in Figures 7−9. Consistent with experimental selectivity trends,[2b] 1_{ch} was found to favor attack at the axial face by LAH, rather than the equatorial face, by 1.1 kcal mol^{-1} (corresponding to an 86:14 ratio of axial:equatorial addition products at 25 °C). The analysis of the geometries of the transition states for attack at the axial and equatorial faces (1_{ch}-TS-LAH$_{ax}$ and 1_{ch}-TS-LAH$_{eq}$, Figure 7) revealed features consistent with the previously described models[6] in which attack on the equatorial face experiences greater torsional strain compared to axial face attack. Although the corresponding "equatorial" and "axial" transition states are located at similar points on the reaction coordinate (the forming C−H and breaking Al−H bond lengths are 1.66 and 1.71 Å, respectively, for both transition structures), addition to the equatorial face of 1_{ch} involves slightly greater eclipsing interactions (ψ = 12° for axial face attack vs 14° for equatorial face attack). Moreover, addition to the chair equatorial face requires greater distortion of the ring dihedral angle relative to the geometry of the reactant 1_{ch} (dihedral angle C−C−C−C = −40° and −60 for 1_{ch}-TS-LAH$_{ax}$ and 1_{ch}-TS-LAH$_{eq}$, respectively, compared to −48° for 1_{ch}). These results illustrate how changes in geometry occurring in the TS region can sometimes have opposing effects: the expansion of a single dihedral angle to optimal values of a C(sp^3)−C(sp^3) bond can be detrimental if it implies a great distortion from the reactant structure. The delicate balance between these stabilizing/destabilizing geometric features ultimately results in the overall relative energies of competing pathways.

The twist-boat transition states for **1** (Figure 7C and 7D) are slightly later (the forming C−H bond length is 1.60 Å for 1_{tb}-TS-LAH and 1.66 Å for 1_{ch}-TS-LAH) and, consequently, higher in energy than the chair transition states for both pro-axial and pro-equatorial hydride addition. This difference in position on the reaction coordinate contributes to amplifying the intrinsic preference for the chair conformation in the transition state ($\Delta\Delta G^{\ddagger}_{twist-chair}$ = 6.2 and 4.7 kcal mol^{-1} for pro-axial and pro-equatorial addition, respectively) with respect to the initial reactant ($\Delta\Delta G_{twist-chair}$ = 2.8 kcal mol^{-1}). The increased destabilization of the twist-boat relative to the chair can also be attributed, at least in part, to a greater difference in torsional strain between the two transition states. The chair conformation gets relief from eclipsing C−O and vicinal C−H bonds upon passing from reactant (dihedral angle O−C−C−H = 8°) to transition state, especially for axial attack (O−C−C−H of 1_{ch}-TS-LAH$_{ax}$ = 45°), albeit with an 8° compression in the C−C−C−C angle. In contrast, the twist-boat transition states maintain an eclipsed arrangement (the smaller O−C−C−H angle = 4° in 1_{tb}, compared to 6−11° in 1_{tb}-TS-LAH). Notably, neither face of the twist boat is strongly preferred for hydride addition by LAH due to similar torsional strain occurring in both approaches, as represented by very similar ψ values. In fact, pro-equatorial attack on the twist boat is slightly favored over pro-axial attack by 0.4 kcal mol^{-1} (Figure 7C and 7D). This weak preference for pro-equatorial attack in the twist boat is opposite to the preference for axial attack on 1_{ch} and alludes to the possibility that stable twist-boat conformations can alter the usual stereoselectivity.

Consistent with literature reports,[9] the equatorial face of piperidone **6** is predicted to be more reactive than the axial face toward LAH by at least 1 kcal mol^{-1} (Figure 8). The predicted stereoselectivity for this reaction, considering all feasible

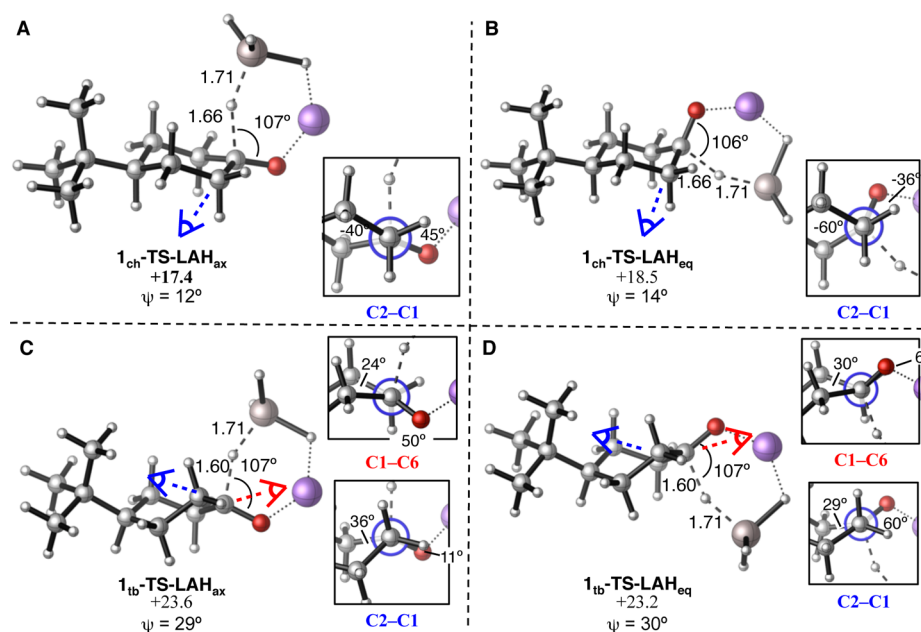| Ketone	Separated Reactants		Coordination Complex		
	ΔG_{chair}	ΔG_{twist}	ΔG_{chair}	ΔG_{twist}	$\Delta\Delta G_{twist-chair}$
1	0.0	+3.2	−11.1	−8.3	+2.8
6	0.0	+0.5	−10.9	−10.2	+0.7
7	0.0	---	−12.3	---	---

Figure 7. Lowest energy transition structures for the addition of LAH to (A) the axial face of **chair 1ch**, (B) the equatorial face of **chair 1ch**, (C) the pro-axial face of **twist-boat 1tb**, and (D) the pro-equatorial face of **twist-boat 1tb**. Optimized structures were calculated at the SMD(THF)/B3LYP/6-311+G(2d,p)//B3LYP/6-31G(d,p) level. Activation Gibbs free energies ($\Delta G^{\ddagger}$) are referenced to the lowest energy prereaction coordination complex and are given in kcal mol^{-1}; distances are given in angstroms and angles in degrees.
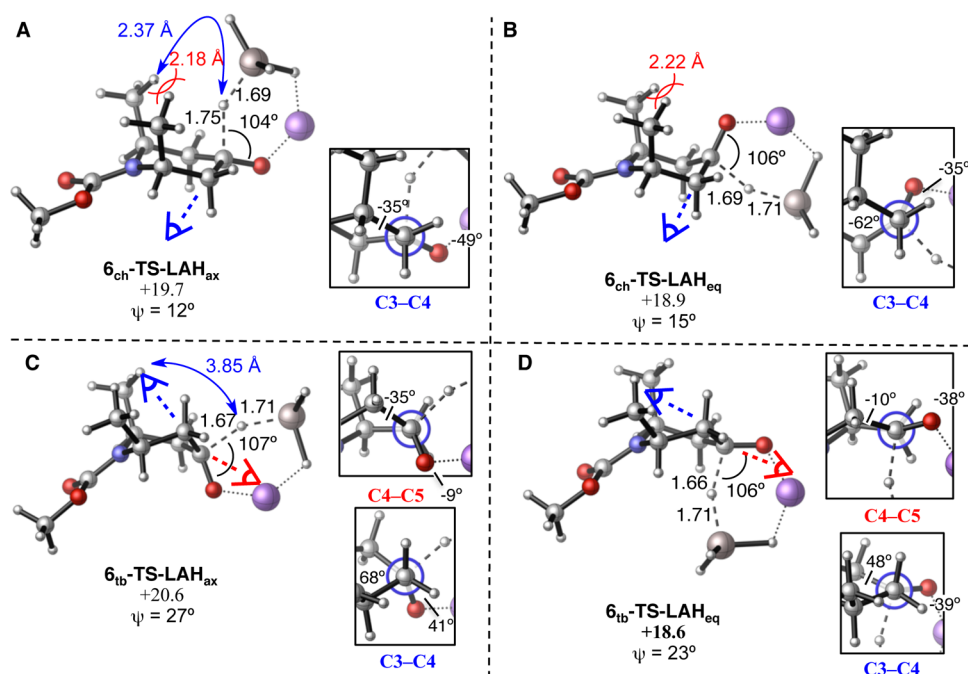

Figure 8. Lowest energy transition structures for the addition of LAH to (A) the axial face of **chair 6ch**, (B) the equatorial face of **chair 6ch**, (C) the pro-axial face of **twist-boat 6tb**, and (D) the pro-equatorial face of **twist-boat 6tb**. Optimized structures were calculated at the SMD(THF)/B3LYP/6-311+G(2d,p)//B3LYP/6-31G(d,p) level. Activation Gibbs free energies ($\Delta G^{\ddagger}$) are referenced to the lowest energy prereaction coordination complex and are given in kcal mol^{-1}; distances are given in angstroms and angles in degrees.

pathways, is a 89:11 ratio of axial:equatorial alcohols at 25 °C (or 95:5 at −78 °C). This equatorial preference is predicted for both chair and twist-boat transition structures ($\Delta\Delta G^{\ddagger}_{eq-ax}$ = −0.8 and −2.0 kcal mol^{-1} for **6ch-TS-LAH** and **6tb-TS-LAH**, respectively). In the chair conformation, the destabilization of the TS for axial face attack is likely caused by the steric hindrance with the 2,6-dimethyl substituents, which translates into a longer forming C−H bond distance (1.75 Å vs 1.66 Å in

the cyclohexanone TS). Attack at the equatorial face of the chair conformation also benefits from a slight mitigation of the 1,3-diaxial interactions between the two methyl groups in the transition state (d_{H-H} = 2.22 Å), while axial attack does not provide any such relief (d_{H-H} = 2.18 Å, compared to 2.19 Å in the reactant). These steric factors override the intrinsically greater torsional strain generated in attack on the equatorial face.
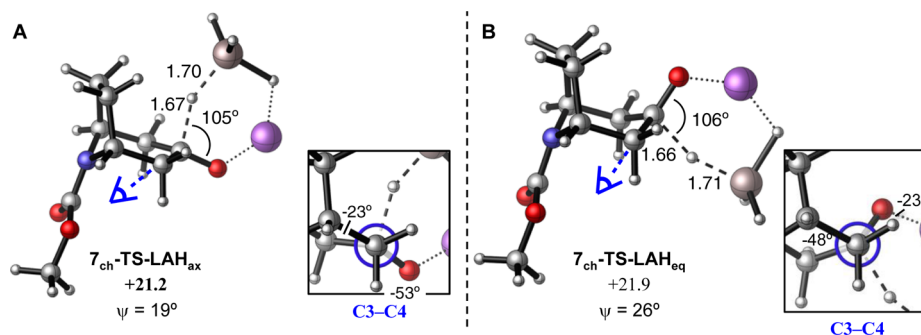
Figure 9. Lowest energy transition structures for the addition of LAH to (A) the axial face of 7_{ch}, and (B) the equatorial face of 7_{ch}. Optimized structures were calculated at the SMD(THF)/B3LYP/6-311+G(2d,p)//B3LYP/6-31G(d,p) level. Activation Gibbs free energies ($\Delta G^{\ddagger}$) are referenced to the lowest energy prereaction coordination complex and are given in kcal mol^{-1}; distances are given in angstroms and angles in degrees.

Consistent with our hypothesis that twist-boat transition states may be involved, pro-equatorial attack on the twist-boat conformation of **6** is not only unusually stable but is even slightly favored (by 0.3 kcal mol^{-1}) over attack on the chair conformation. In fact, 6_{tb}-**TS-LAH**$_{eq}$ was calculated to be the lowest energy pathway for the addition of LAH to **6**. The trajectory of hydride addition to the pro-axial face of 6_{tb} is remote from the 2,6-dimethyl substituents (d_{H-H} = 3.85 Å in 6_{tb}-**TS-LAH**$_{ax}$). Nevertheless, pro-equatorial attack on the twist-boat is preferred, and is ~5 kcal mol^{-1} lower than that of the twist-boat transition state of cyclohexanone **1**.

Figure 9 shows the transition states for reaction of tropinone **7** with LAH. Consistent with its experimentally observed reactivity,[11] and contrary to its nonbridged analogue **6**, tropinone **7** is predicted to undergo preferential hydride attack by LAH at the axial face (typical Felkin–Anh selectivity), although with a lower stereoselectivity ($\Delta\Delta G^{\ddagger}_{eq-ax}$ = +0.7 kcal mol^{-1}, leading to a 85:15 ratio of equatorial:axial alcohols at −78 °C). Steric hindrance in the axial addition trajectory of 7_{ch}-**TS-LAH**$_{ax}$ is slightly less important, since the AlH$_4$ approaches somewhat further away from the ethylene bridge in **7** than from the dimethyls of piperidone **6**. Also, the advantage of alleviating the 1,3-diaxial interactions described for the equatorial attack in 6_{ch} and both approaches in 6_{tb} does not apply to 7_{ch}, in which these substituents are bridged. The geometric constraints imposed by the bicyclic structure of 7_{ch} preclude relaxation of the torsional strain generated in the transition states, as reflected by the activation barriers that are calculated to be 2−4 kcal mol^{-1} higher for **7** than for **6** and **1** and by the 7−12° increase in the ψ values for **7** with respect to **6** and **1**. In view of the different stereochemical outcomes observed for the addition of LAH to piperidone **6** and tropinone **7**, it can be concluded that relaxation of 1,3-diaxial interactions, either by accessing twist-boat conformations or by favoring equatorial addition trajectories, is the key factor determining facial stereoselectivity in the reduction of this type of system with small hydrides, overriding the contribution of other steric factors.

Reactions with a Bulky Nucleophile (LTBH). As observed with LAH, all three substrates studied form prereaction coordination complexes with lithium triisopropyl-borohydride (LTBH) that are lower in energy than the separated reactants (see, for example, Figure 10A). The activation energies reported here for reduction with LTBH are also measured from the lowest-energy prereaction coordination complexes. For **1**, the difference in energy between chair and twist-boat conformations is essentially
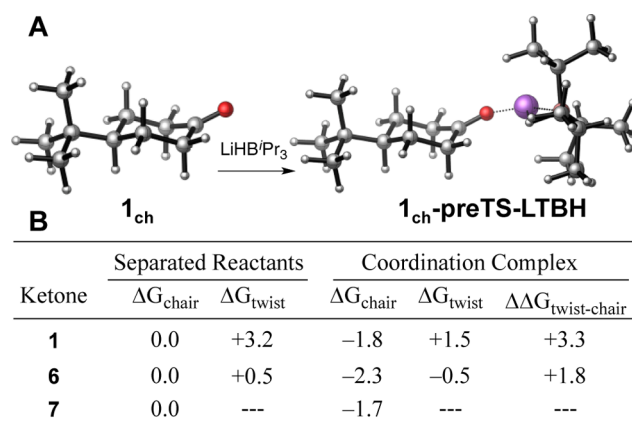

Figure 10. (A) Example of formation of the reactant complex with LTBH, shown for 1_{ch}. (B) Comparison of the Gibbs free energies (ΔG) of chair and twist-boat conformations of free ketones **1**, **6**, and **7** and their prereaction complexes with LTBH. Optimized structures were calculated at the SMD(THF)/B3LYP/6-311+G(2d,p)//B3LYP/6-31G(d,p) level. Gibbs free energies (ΔG) are referenced to the lowest energy free ketone conformation and are given in kcal mol^{-1}.

conserved upon formation of the prereaction complex (Figure 10B). However, for piperidone **6**, the twist-boat conformation is destabilized relative to the chair upon formation of the prereaction complex ($\Delta\Delta G_{twist-chair}$ = 1.8 kcal mol^{-1} for the prereaction complexes vs 0.5 kcal mol^{-1} for the uncomplexed ketone conformations, respectively).

The bulky hydride reagent is less reactive than the sterically less-demanding reagent LAH, as reflected by higher overall activation barriers calculated for LTBH. The reactivity trend observed for the three cyclic ketones toward LAH is maintained for reduction with LTBH, although the differences in the calculated activation energies are smaller ($\Delta G^{\ddagger}$ = 24.7, 24.9, and 25.3 kcal mol^{-1} for **1**, **6**, and **7**, respectively; Figures 11−13). Both the lithium and the potassium salts of Selectride are commonly used experimentally as a bulky hydride reagents. Therefore, we also investigated the reactivity of piperidone **6** and tropinone **7** toward potassium triisopropylborohydride (KTBH), in addition to LTBH. The corresponding calculated activation energies indicate a somewhat greater reactivity of KTBH with respect to LTBH ($\Delta G^{\ddagger}$ = 22.9 and 25.1 kcal mol^{-1} for the reaction of KTBH with **6** and **7**, respectively).[17] This may be due to a weaker interaction between K$^+$ and the incoming hydride in the transition structure, as suggested by the computed transition state geometries. The calculated
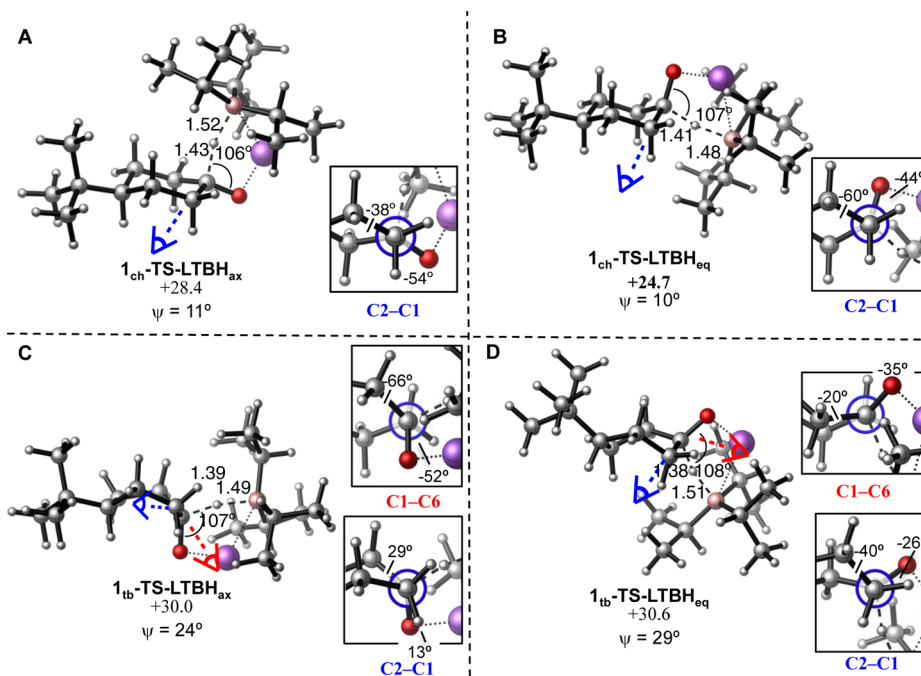
Figure 11. Lowest energy transition structures for the addition of LTBH to (A) the axial face of **chair 1_ch**, (B) the equatorial face of **chair 1_ch**, (C) the pro-axial face of **twist-boat 1_tb**, and (D) the pro-equatorial face of **twist-boat 1_tb**. Optimized structures were calculated at the SMD(THF)/B3LYP/6-311+G(2d,p)//B3LYP/6-31G(d,p) level. Activation Gibbs free energies ($\Delta G^{\ddagger}$) are referenced to the lowest energy prereaction coordination complex and are given in kcal mol^{-1}; distances are given in angstroms and angles in degrees.
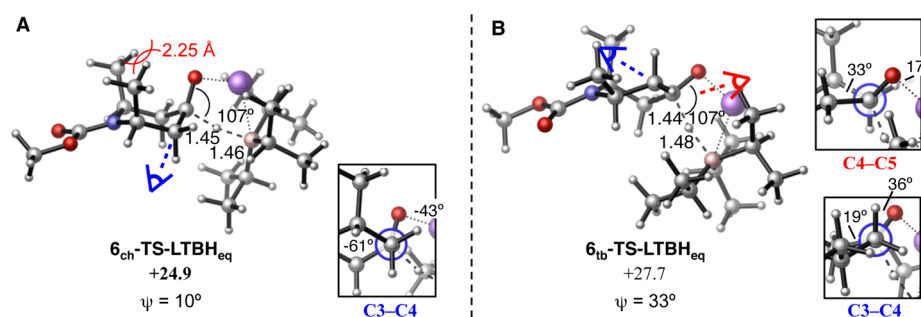

Figure 12. Lowest energy transition structures for the addition of LTBH to (A) the equatorial face of **chair 6_ch** and (B) the pro-equatorial face of **twist-boat 6_tb**. Optimized structures were calculated at the SMD(THF)/B3LYP/6-311+G(2d,p)//B3LYP/6-31G(d,p) level. Activation Gibbs free energies ($\Delta G^{\ddagger}$) are referenced to the lowest energy prereaction coordination complex and are given in kcal mol^{-1}; distances are given in angstroms and angles in degrees.

transition structures are earlier with K$^+$ than with Li$^+$. The kinetic preference for **6** vs **7** predicted by our calculations is consistent with the results of the competition experiment described in Scheme 2. Due to the very similar chair vs twist-boat selectivity trends calculated for LTBH and KTBH ($\Delta\Delta G^{\ddagger}_{twist-chair}$ = 2.8 and 2.6 kcal mol^{-1} for the reaction of **6** with LTBH and KTBH, respectively), and to facilitate a more direct comparison to LAH, we will only discuss the reactivity of LTBH hereafter. A more detailed description of the reactivity of KTBH with **6** and **7** can be found in the Supporting Information.

In accordance with experimental results,[3,9,11] the three substrates studied are consistently predicted to prefer attack at the equatorial face by the bulky hydride reagent LTBH. Despite the large number of conformers accessible for each productive reaction pathway (e.g., 108 conformers representing approach of LTBH to just one face of **6**), in all cases reaction with LTBH proceeds through significantly later transition states

(forming d_{C-H} = 1.38−1.45 with LTBH vs 1.66−1.75 Å with LAH, Figure 11−13).

LTBH favors addition to the equatorial face of **1_ch** by 3.7 kcal mol^{-1} (Figure 11A and 11B). The transition states are late, and the carbonyl carbon is nearly tetrahedral. Thus, the surrounding dihedral angles in the chair TS are more staggered than in the transition structures with LAH. This feature is reflected in the slightly smaller values of ψ for the chair TS with LTBH (ψ = 10−11°) vs with LAH (ψ = 12−14°). Furthermore, the difference in torsional strain between attack at the axial and equatorial faces (range of ψ values) with LTBH is smaller than with LAH, rendering torsional strain less influential on facial selectivity of these chair TS.

Only a small energy difference is calculated between the transition states for reaction at the two faces of the twist boat with LTBH ($\Delta\Delta G^{\ddagger}_{eq-ax}$ = +0.6 kcal mol^{-1}). Addition to either face of the twist boat is prohibitively high in energy relative to the favored addition to the equatorial face of **1_ch** ($\Delta\Delta G^{\ddagger}_{twist-chair}$ ~6 kcal mol^{-1} for pro-equatorial addition, Figure 11D vs 11B).

Due to exceedingly large steric repulsions between LTBH and the substrate 2,6-substituents, only equatorial-face addition transition structures could be located for the reaction of piperidone **6** (Figure 12) and tropinone **7** (Figure 13) with this
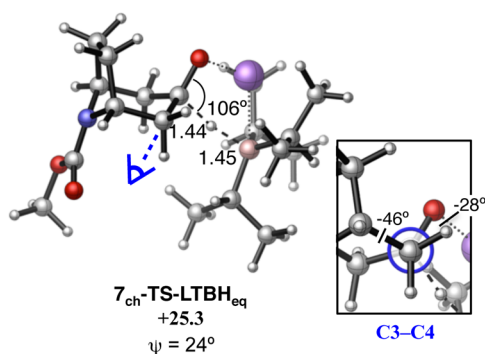

Figure 13. Lowest energy transition structure for the addition of LTBH to the equatorial face of **7**$_{ch}$. Optimized structures were calculated at the SMD(THF)/B3LYP/6-311+G(2d,p)//B3LYP/6-31G(d,p) level. Activation Gibbs free energy ($\Delta G^{\ddagger}$) is referenced to the lowest energy prereaction coordination complex and is given in kcal mol^{-1}; distances are given in angstroms and angles in degrees.

bulky hydride reagent.[18] The energetic degeneracy predicted for the pro-equatorial addition of LAH to both the chair and twist-boat conformations of **6** is not conserved with LTBH, for which the twist-boat transition state is disfavored by ~3 kcal mol^{-1} due to a simultaneous reduction in the torsional strain of **6**$_{ch}$-**TS-LTBH**$_{eq}$ ($\psi = 10°$) and increase in torsional strain of **6**$_{tb}$-**TS-LTBH**$_{eq}$ ($\psi = 33°$). Taken together with the results using LAH, these studies show that twist-boat conformations can be relevant for both reactivity and selectivity of cis-2,6-disubstituted piperidones for reduction by *small* hydride reagents but not with LTBH or, presumably, other bulky nucleophiles.

CONCLUSIONS

The computational results described in this paper are consistent with the Felkin–Anh model for predicting the facial selectivity of the reaction of *tert*-butylcyclohexanone **1** and tropinone **7** with a small hydride reagent: LAH preferentially adds to the axial face of both **1** and **7**. An exception to this common trend is found in piperidone **6**, for which a twist-boat conformation is calculated to be relevant to the transition state for addition of a small hydride reagent, and pro-equatorial attack by LAH is overall preferred. Our results indicate that pro-equatorial attack on a twist-boat (i.e., attack at the face that would lead to an equatorial nucleophile in the chair conformation of the product) with a small nucleophile does not necessarily incur more torsional strain than pro-axial attack. Additionally, our calculations show that the torsional strain developed during both attack on the axial and equatorial faces of a chair depends also on the nature of the incoming nucleophile. With a bulky hydride, the degree of torsional strain experienced in the transition states for attack at the equatorial and axial faces are similar, and selectivity is dominated by steric effects.

EXPERIMENTAL SECTION

General Information. All synthetic reactions described in this paper were performed using oven-dried glassware under an argon or dry nitrogen atmosphere. THF, toluene, and diethyl ether were dried by distillation from sodium/benzophenone. Other reagents and

solvents were stored over molecular sieves under argon and used directly. Radial PLC was performed using a model 7924T Chromatotron using thin layers of silica gel−gypsum. Melting points were measured using a capillary melting point apparatus. The mass analyzer type used for the HRMS measurements was TOF with electrospray as the ionization method. NMR spectra were obtained using a 300 or 400 MHz spectrometer. Chemical shifts are in δ units (ppm) with TMS (0.0 ppm) used as an internal standard for ^{1}H NMR spectra and the CDCl$_3$ absorption at 77.23 ppm for ^{13}C NMR.

cis-N-(Phenoxycarbonyl)-2,6-dimethyl-4-piperidone (3). To CuBr·SMe$_2$ (177 mg, 0.86 mmol) in DMS (4 mL) at −78 °C was added MeLi (1.4M/Et$_2$O, 1.23 mL, 1.72 mmol). The reaction mixture was allowed to warm to −30 °C over 30 min and then cooled to −78 °C. A solution of N-(phenoxycarbonyl)-2-methyl-2,3-dihydropyridone (100 mg, 0.43 mmol) in 0.5 mL of DMS was added via syringe. The mixture was stirred at −78 °C for 3 h and then at −42 °C for 30 min. The cooling bath was removed and saturated aqueous NH$_4$Cl (0.5 mL) was added followed by anhydrous Na$_2$SO$_4$ (~8 g). After stirring for 2 h, the mixture was filtered and concentrated to give the crude product. Purification by radial PLC (SiO$_2$, 10−20% EtOAc/hexanes) afforded 91 mg (85%) of **3** as a clear oil (product contains ~7% of the trans isomer). IR (neat) 2974, 1710, 1336, 1204 cm^{-1}; ^{1}H NMR (300 MHz, CDCl$_3$) δ 7.36 (m, 2H), 7.2 (m, 1H), 7.11 (d, 2H, J = 8.4 Hz), 4.90 (m, 2H), 2.79 (dd, 2H, J = 7.6, 15.1 Hz), 2.38 (dd 2H, J = 2.1, 15.0 Hz), 1.38 (d, 6H, J = 7.0 Hz); ^{13}C NMR (75 MHz, CDCl$_3$) δ 207.9, 154.0, 151.4, 129.6, 125.7, 121.9, 49.5, 45.5, 23.2; HRMS calcd for C$_{14}$H$_{17}$NO$_3$ [(M + H)$^+$] 248.1281, found 248.1275.

cis-N-(Phenoxycarbonyl)-2,6-dimethyl-4-piperidinol (3a). To a solution of piperidone **3** in THF (2 mL) at −78 °C was added K-Selectride (1 M/THF, 0.33 mL, 0.33 mmol), and the mixture was stirred at −78 °C for 1 h. Anhydrous acetone (0.3 mL) was added, and stirring was continued for 5 min. The cooling bath was removed, saturated NH$_4$Cl (0.5 mL) added, and the mixture stirred at rt for 1 h. EtOAc (15 mL) and dry Na$_2$SO$_4$ (~3 g) were added. After stirring for 1 h, filtration and concentration gave the crude product. Purification by radial PLC (SiO$_2$, EtOAc/hexanes) afforded 63 mg (84%) of alcohol **3a** as a white solid, mp 127−128 °C (10% EtOAc/hexanes). IR (neat) 3466, 2967, 1710, 1688; ^{1}H NMR (300 MHz, CDCl$_3$) δ 7.33 (t, 2H, J = 8.4 Hz), 7.19 (t, 1H, J = 8.4 Hz), 7.1 (d, 2H, J = 8.4 Hz), 4.46 (m, 2H), 4.0 (m, 1H), 2.28 (s, 1H), 2.06 (m, 2H), 1.62 (m, 2H), 1.46 (d, 6H, J = 6.6 Hz); ^{13}C NMR (75 MHz, CDCl$_3$) δ 154.3, 151.6, 129.5, 125.4, 122.0, 65.1, 46.8, 37.1, 24.0; HRMS calcd for C$_{14}$H$_{19}$NO$_3$ [(M + H)$^+$] 250.1438, found 250.1433.

Reduction of Piperidone Mixture (3 and 5). *Competition Study.* To a 50/50 mixture of piperidones **3** (0.12 mmol) and **5** (0.12 mmol) in THF (3 mL) at −74 °C was added K-selectide (1 M/THF, 0.12 mL, 0.12 mmol) dropwise. The mixture was stirred for 1 h at −72 to −74 °C. Anhydrous acetone (0.2 mL) was added, and stirring was continued for 5 min. The cooling bath was removed, saturated aqueous NH$_4$Cl (0.5 mL) added, and the mixture stirred for 1 h at room temperature. EtOAc (10 mL) and anhydrous Na$_2$SO$_4$ (~4 g) were added. After stirring for 1 h, filtration and concentration gave the crude product. Analysis by HPLC and NMR showed that the ketones **3** and **5** were reduced in a ratio of 75:25 (see Supporting Information).

Computational Details. All geometry optimizations were carried out with the B3LYP hybrid functional[19,20] and 6-31G(d,p) basis set. Calculations were carried out with Gaussian 09.[21] Single-point energy calculations were performed on the optimized geometries using the 6-311+G(2d,p) basis set. The meta-hybrid M06-2X[22] functional was also tested for both geometry optimization and single-point energy calculations, using the same basis sets described above. Similar results were obtained with both methods, although the B3LYP functional showed a better agreement with experimental results. The theoretical ratio of reaction products was obtained through the Gibbs free energy of the different transition states ($\Delta G^{\ddagger}$) using a Maxwell−Boltzmann distribution at the appropriate temperature. Thermal and entropic corrections to energy were calculated from vibrational frequencies. The nature of the stationary points was determined in each case according to the appropriate number of negative eigenvalues of the Hessian matrix from the frequency calculations. Scaled frequencies

were not considered, because significant errors in the calculated thermodynamic properties are not found at this theoretical level.[23,24] Mass-weighted intrinsic reaction coordinate (IRC) calculations were carried out using the Gonzalez and Schlegel scheme[25,26] to ensure that the TSs indeed connect the appropriate reactants and products. Bulk solvent effects were considered implicitly by performing single-point energy calculations on the gas-phase optimized geometries, through the SMD polarizable continuum model of Cramer and Truhlar[27] as implemented in Gaussian 09. The parameters for tetrahydrofuran were used to calculate solvation free energies (ΔG_{solv}). Cartesian coordinates, electronic energies, entropies, enthalpies, Gibbs free energies, and lowest frequencies of the different conformations of all structures are available as Supporting Information.

■ ASSOCIATED CONTENT

ⓢ Supporting Information

Additional figures, compound characterization, Cartesian coordinates, electronic energies, entropies, enthalpies, Gibbs free energies, and lowest frequencies of the calculated structures (lowest energy conformers). This material is available free of charge via the Internet at http://pubs.acs.org.

■ AUTHOR INFORMATION

Corresponding Authors
*E-mail: houk@chem.ucla.edu.
*E-mail: gjimenez@chem.ucla.edu.
*E-mail: daniel_comins@ncsu.edu.
Notes
The authors declare no competing financial interest.

■ ACKNOWLEDGMENTS

■ REFERENCES

(1) For reviews, see (a) Gung, B. W. *Chem. Rev.* **1999**, *99*, 1377−1386. (b) Greeves, N. *Comprehensive Organic Synthesis*; Trost, B. M.; Fleming, I., Eds.; Pergamon Press: Oxford, 1991; Vol. 8, p 1.
(2) (a) Novak, M.; Gung, B. W.; Hershberger, J. W.; Taylor, R. T.; Emenike, B.; Chakraborty, M.; Scioneaux, A. N.; Ponsot, A. E.; Daka, P. *Chem. Educator* **2009**, *14*, 232−235. (b) Eliel, E. L.; Rerick, M. N. *J. Am. Chem. Soc.* **1960**, *82*, 1367−1372.
(3) (a) Brown, H. C.; Krishnamurthy, S. *J. Am. Chem. Soc.* **1972**, *94*, 7159−7161. (b) Gärtner, P.; Novak, C.; Knollmüller, M.; Gmeiner, G. *ARKIVOC* **2001**, No. ii, 9−20.
(4) (a) Dauben, W. C.; Fonken, G. J.; Noyce, D. S. *J. Am. Chem. Soc.* **1956**, *78*, 2579−2582. (b) Gung, B. W. *Tetrahedron* **1996**, *52*, 5263−5301.
(5) (a) Chérest, M.; Felkin, H.; Prudent, N. *Tetrahedron Lett.* **1968**, *9*, 2199−2204. (b) Cherest, M.; Felkin, H. *Tetrahedron Lett.* **1971**, 383−386. (c) Anh, N. T.; Eisenstein, O.; Lefour, J.-M.; Tran Huu Dau, M.-E. *J. Am. Chem. Soc.* **1973**, *95*, 6146−6147.
(6) (a) Wu, Y.-D.; Houk, K. N. *J. Am. Chem. Soc.* **1987**, *109*, 908−910. (b) Wu, Y.-D.; Houk, K. N.; Trost, B. M. *J. Am. Chem. Soc.* **1987**, *109*, 5560−5561. (c) Mukherjee, D.; Wu, Y.-D.; Fronczek, F. R.; Houk, K. N. *J. Am. Chem. Soc.* **1988**, *110*, 3328−3330. (d) Wu, Y.-D.; Tucker, J. A.; Houk, K. N. *J. Am. Chem. Soc.* **1991**, *113*, 5018−5027. (e) Wu, Y.-D.; Houk, K. N.; Paddon-Row, M. N. *Angew. Chem., Int. Ed.* **1992**, *31*, 1019−1021. (f) Paddon-Row, M. N.; Wu, Y.-D.; Houk, K. N. *J. Am. Chem. Soc.* **1992**, *114*, 10638−10639. (g) Ando, K.; Houk, K. N.; Busch, J.; Menassé, A.; Séquin, U. *J. Org. Chem.* **1998**, *63*, 1761−1766.

(7) (a) Wipke, W. T.; Gund, P. *J. Am. Chem. Soc.* **1976**, *98*, 8107−8118. (b) Perlburger, J. C.; Müller, P. *J. Am. Chem. Soc.* **1977**, *99*, 6316−6319. (c) Frenking, G.; Köhler, K. F.; Reetz, M. T. *Angew. Chem., Int. Ed.* **1991**, *30*, 1146−1149. (d) Coxon, J. M.; Luibrand, R. T. *Tetrahedron Lett.* **1993**, *34*, 7097−7100. (e) Luibrand, R. T.; Taigounov, I. R.; Taigounov, A. A. *J. Org. Chem.* **2001**, *66*, 7254−7262.
(8) (a) Cieplak, A. S. *J. Am. Chem. Soc.* **1981**, *103*, 4550. (b) Cieplak, A. S.; Tait, B. D.; Johnson, C. R. *J. Am. Chem. Soc.* **1989**, *111*, 8447.
(9) (a) Comins, D. L.; Dehghani, A. *J. Chem. Soc., Chem. Commun.* **1993**, 1838−1839. (b) Comins, D. L.; Dehghani, A. *J. Org. Chem.* **1995**, *60*, 794−795. (c) Comins, D. L.; LaMunyon, D. H.; Chen, X. *J. Org. Chem.* **1997**, *62*, 8182−8187. (d) Kuethe, J. T.; Comins, D. L. *J. Org. Chem.* **2004**, *69*, 5219−5231. (e) McCall, W. S.; Grillo, T. A.; Comins, D. L. *Org. Lett.* **2008**, *20*, 3255−3257. (f) McCall, W. S.; Comins, D. L. *Org. Lett.* **2009**, *11*, 2940−2942. (g) Guo, F.; Dhakal, R. C.; Dieter, R. K. *J. Org. Chem.* **2013**, *78*, 8451−8464.
(10) The axial orientation of the 2,6-substituents is preferred to avoid allylic strain induced by the *N*-acetyl group; see ref 15 for NMR and crystallographic support in favor of this diaxial configuration, as well as the following review: Johnson, F. *Chem. Rev.* **1968**, *68*, 375−413.
(11) (a) Nagase, T.; Takahashi, T.; Sasaki, T.; Nagumo, A.; Shimamura, K.; Miyamoto, Y.; Kitazawa, H.; Kanesaka, M.; Yoshimoto, R.; Aragane, K.; Tokito, S.; Sato, N. *J. Med. Chem.* **2009**, *52*, 4111−4114. (b) Xia, Y.; Chackalamannil, S.; Greenlee, W. J.; Jayne, C.; Neustadt, B.; Stamford, A.; Vaccaro, H.; Xu, X.; Baker, H.; O'Neill, K.; Woods, M.; Hawes, B.; Kowalski, T. *Bioorg. Med. Chem. Lett.* **2011**, *21*, 3290−3296.
(12) The participation of reactive twist-boat conformations in reductions of cyclohexanones has previously been suggested: Landor, S. R.; Regan, J. P. *J. Chem. Soc. C* **1967**, 1159−1163.
(13) Additional examples of steric repulsions overcoming torsional strain have been described; for a recent review, see: Wang, H.; Houk, K. N. *Chem. Sci.* **2014**, *5*, 462−470.
(14) Tri-*sec*-butylborohydride (Selectride) has up to 5832 conformations: Each *sec*-butyl has two relevant rotatable C(sp^3)−C(sp^3) bonds, or $3^2 = 9$ rotamers. Taking into account all combinations of rotamers of all three *sec*-butyl groups, there are $9^3 = 729$ rotamers possible for any given stereoisomer of Selectride. Selectride has three chiral centers, and thus eight possible stereoisomers; $729 \times 8 = 5832$.
(15) (a) Venkatraj, M.; Ponnuswamy, S.; Jeyaraman, R. *Indian J. Chem.* **2008**, *47B*, 411−426. (b) Ponnuswamy, S.; Venkatraj, M.; Jeyaraman, R. *Indian J. Chem.* **2002**, *41B*, 614−627. (c) Jeyaraman, R.; Ponnuswamy, S. *Indian J. Chem.* **1997**, *36B*, 730−737.
(16) Guo, F.; Dhakal, R. C.; Dieter, R. K. *J. Org. Chem.* **2013**, *78*, 8451−8464.
(17) Because explicit solvation by THF is not considered in these calculations due to their complexity, some error is expected when comparing transition state energies involving different metal cations (Li$^+$ vs K$^+$), which may coordinate solvent differently.
(18) In these cases, attempts to locate transition structures for axial addition of the bulky hydride failed to converge during geometry optimizations.
(19) Lee, C.; Yang, W.; Parr, R. G. *Phys. Rev. B* **1988**, *37*, 785−789.
(20) Becke, A. D. *J. Chem. Phys.* **1993**, *98*, 5648−5652.
(21) Frisch, M. J.; Trucks, G. W.; Schlegel, H. B.; Scuseria, G. E.; Robb, M. A.; Cheeseman, J. R.; Scalmani, G.; Barone, V.; Mennucci, B.; Petersson, G. A.; Nakatsuji, H.; Caricato, M.; Li, X.; Hratchian, H. P.; Izmaylov, A. F.; Bloino, J.; Zheng, G.; Sonnenberg, J. L.; Hada, M.; Ehara, M.; Toyota, K.; Fukuda, R.; Hasegawa, J.; Ishida, M.; Nakajima, T.; Honda, Y.; Kitao, O.; Nakai, H.; Vreven, T.; Montgomery, J.; Peralta, J. E.; Ogliaro, F.; Bearpark, M.; Heyd, J. J.; Brothers, E.; Kudin, K. N.; Staroverov, V. N.; Kobayashi, R.; Normand, J.; Raghavachari, K.; Rendell, A.; Burant, J. C.; Iyengar, S. S.; Tomasi, J.; Cossi, M.; Rega, N.; Millam, J. M.; Klene, M.; Knox, J. E.; Cross, J. B.; Bakken, V.; Adamo, C.; Jaramillo, J.; Gomperts, R.; Stratmann, R. E.; Yazyev, O.; Austin, A. J.; Cammi, R.; Pomelli, C.; Ochterski, J. W.; Martin, R. L.; Morokuma, K.; Zakrzewski, V. G.; Voth, G. A.; Salvador, P.; Dannenberg, J. J.; Dapprich, S.; Daniels, A. D.; Farkas, Ö.;

Foresman, J. B.; Ortiz, J. V.; Cioslowski, J.; Fox, D. J. *Gaussian 09*, Gaussian, Inc., Wallingford, CT, 2009.

(22) Zhao, Y.; Truhlar, D. *Theor. Chem. Acc.* **2008**, *120*, 215−241.

(23) Bauschlicher, C. W., Jr. *Chem. Phys. Lett.* **1995**, *246*, 40−44.

(24) Merrick, J. P.; Moran, D.; Radom, L. *J. Phys. Chem. A* **2007**, *111*, 11683−11700.

(25) Gonzalez, C.; Schlegel, H. B. *J. Chem. Phys.* **1989**, *90*, 2154−2161.

(26) Gonzalez, C.; Schlegel, H. B. *J. Phys. Chem.* **1990**, *94*, 5523−5527.

(27) Marenich, A. V.; Cramer, C. J.; Truhlar, D. G. *J. Phys. Chem. B* **2009**, *113*, 6378−6396.